

## Investigation of the triggering process of pellet induced ELMs

G. Kocsis<sup>1</sup>, S. Kálvin<sup>1</sup>, P.T. Lang<sup>2</sup>, M. Maraschek<sup>2</sup>, W. Schneider<sup>2</sup>,  
T. Szepesi<sup>1</sup> and ASDEX Upgrade Team

<sup>1</sup> *KFKI-Research Institute for Particle and Nuclear Physics, EURATOM Association, P.O.Box 49, H-1525 Budapest-114, HUNGARY*

<sup>2</sup> *Max-Planck-Institut für Plasmaphysik, EURATOM Association, Boltzmannstr. 2, 85748 Garching, GERMANY*

The transient power load on plasma facing components caused by edge localized modes (ELMs) in H-mode plasmas can be critically high for large size toroidal machines like ITER, therefore it is of high importance to develop methods to mitigate its effect by external pacing. In the last decade several methods (rapid oscillations of the vertical position of the plasma [1], intermittent gas injection [2], pellet injection [3]) have been investigated, and the injection of frequent small and shallow penetrating cryogenic pellets have been found to be a promising technique. This technique works but the underlying physical processes of the ELM triggering are not well understood, therefore our aim is to study how and where a pellet triggers an ELM.

The major questions to be answered are: at which magnetic surface is the ELM initiated, and what is the corresponding local perturbation caused by the ablating pellet. To obtain answers the pellet parameters (velocity and mass) are varied, and the onset of MHD footprint of the triggered ELMs detected by magnetic pick up coils and the MHD energy loss of the plasma caused by the ELM collapse are measured.

In our investigations - as a working hypothesis - we suppose that to trigger an ELM the pellet has to reach a certain magnetic surface of the plasma (location of the seed perturbation) inside the separatrix independently of its mass and velocity. After the pellet reached this surface, the perturbation introduced by the ablating pellet spreads and finally an instability starts to grow which develops into an ELM. If it reaches the detection threshold we can observe it e.g. by using magnetic pick up coils. As a consequence of this hypothesis, the triggered ELM is delayed after the pellet entered into the plasma. The delay time has two components. One is a time of flight of the pellet to the location of the seed perturbation, and the other is an intrinsic delay which incorporates the perturbation spread time and the instability growth time. The time of flight can be ruled out by performing a pellet velocity scan and therefore the location of the seed perturbation and the intrinsic delay time can be determined.

The experiments - described in this paper - were performed on the ASDEX Upgrade tokamak. Pellets were injected from the high field side of the torus into the type-I ELM regime of an H-mode discharge. In order to avoid the disturbance of the natural ELM cycle and parasitic plasma fueling, perturbative ELM triggering with driving frequency (6Hz) small compared to the natural ELM frequency (25-45 Hz) was used. In this way ELMs were randomly triggered at different times elapsed after the previous natural ELM ( $dt_{elapsed}$ ) therefore the analysis was performed as a function of  $dt_{elapsed}$ .

To rule out the time of flight effect, pellets with four different velocities (240, 600, 880 and 1000 m/s) were used in the investigations. Depending on the pellet velocity the originally identical pellet size was eroded in the HFS looping system [4], resulting in the following pellet radius (and deuterium content) before entering the plasma: 240m/s: 0.71mm ( $9 \cdot 10^{19}$ ), 600m/s: 0.67mm ( $7.4 \cdot 10^{19}$ ), 880m/s: 0.58mm ( $9 \cdot 5^{19}$ ), 1000m/s: 0.51mm ( $3.3 \cdot 10^{19}$ ).

We want to measure the delay of a triggered ELM relative to the pellet injection therefore a reference time - the time when the pellet crossed the separatrix - was selected. To calculate this time the pellet trajectory was reconstructed for every individual pellet using tangentially viewing digital cameras [5]. For the determination of the separatrix the 'Reconstruction of magnetic equilibrium with CLISTE Code' [6] is used.

To get information about the dynamics of the pellet triggered ELMs, the evolution of their MHD activity was monitored by a set of magnetic pick-up coils located about 10cm from the separatrix in the scrape off layer of ASDEX Upgrade [7]. It consists of 14 printed circuit coils measuring the variation of the radial magnetic field component. The coils are located on the low field side of the vessel, covering a poloidal angle of approximately  $60^\circ$  (centered on the outer equatorial line (7 coils) and located toroidally about  $210^\circ$  from the poloidal cross section of the pellet injection) and a toroidal angle of approximately  $180^\circ$  near to the equatorial plane (5 coils). They are particularly suited for the study of the high frequency MHD phenomena related to the ELM cycle, where short timescales are expected as well as high poloidal mode numbers.

Additionally a set of Mirnov coils installed on the inner wall of the AUG vacuum vessel covering a complete poloidal 'circle' (30 coils) was also used to detect the ELM onset [8]. These coils are located about  $190^\circ$  toroidally from the pellet injection.

Analyzing the signal of the magnetic pick-up coils, it was observed that at the very beginning of the ELM event (either a natural or a triggered one) a strong quasi periodic oscillation can be seen on all channels starting at the same time within  $\pm 10\mu s$ . For the applied plasma scenario this oscillation fell into a frequency range of 100 – 300kHz. To get the time evolution of the oscillation amplitude, the Hilbert-Huang spectrogram of the signal was calculated [9]. The advantage of the use of the Hilbert-Huang spectrogram is that this transformation provides the amplitude of any oscillation without significant smoothing which would deteriorate the time resolution. In order to eliminate other non ELM related phenomena, the spectrogram was integrated in the above frequency range and the result is considered as the magnitude of the ELM related MHD activity. The ELM onset was defined as the time when the magnitude exceeds a predefined threshold.

The ELM onset time was calculated for every pellet triggered ELM and for every coil. The poloidal pick-up coil set was used to define a reference ELM onset time for each ELM by averaging the onset times calculated for these coils. The time difference between the onset times and the reference ELM onset time for every triggered ELM and coil can be seen on Fig.1. for shot 20043. It is obvious, that the ELM onset times obtained from the magnetic pick-up coil signals differ from the reference ELM onset time only with about  $\pm 10\mu s$  that is the ELMs can be detected at the same time on all pick-

up coil signals (Fig.1.a. and Fig.1.b.). It also justifies the further use of the reference ELM onset time with a  $\pm 10\mu s$  error. The situation is nearly the same for the poloidal Mirnov coil set (Fig.1.c.), but the ELM onset can be detected significantly earlier on the coils located on the HFS close to the equatorial plane (for poloidal angle between  $150^\circ$  and  $210^\circ$ ). Having a closer look for the raw signals it seems that an oscillation and/or changes can already be seen a few tens of a microsecond before the reference ELM onset time, but after the time when the pellet crossed the separatrix. The origin of this observation is not yet clear. It may be the consequence of the magnetic field perturbation caused by the high beta pellet cloud.

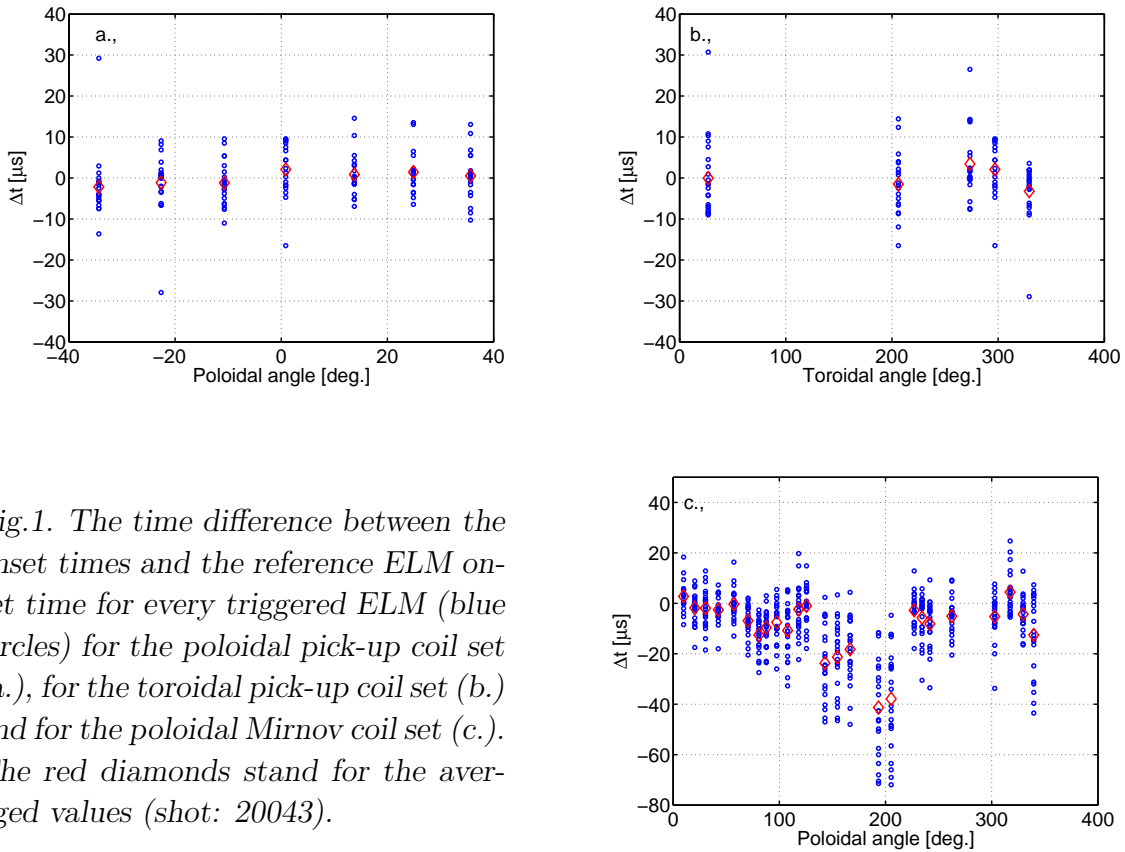


Fig.1. The time difference between the onset times and the reference ELM onset time for every triggered ELM (blue circles) for the poloidal pick-up coil set (a.), for the toroidal pick-up coil set (b.) and for the poloidal Mirnov coil set (c.). The red diamonds stand for the averaged values (shot: 20043).

The delay between the reference ELM onset time and the time when the pellet crossed the separatrix (ELM onset delay:  $dt_{ELM\_ONSET}$ ) was calculated for pellet triggered ELMs for a series of discharges with the mentioned pellet injection scenarios. It is clear that pellets can trigger ELMs at any time in the ELM cycle, that is the plasma edge is not stable against a pellet induced seed perturbation. It was observed that ELM onset delay is nearly constant if the elapsed time ( $dt_{elapsed}$ ) is larger than 8ms, and increases for shorter elapsed times. On the other hand the ELM onset delay was found to be independent of the pellet mass.

According to our assumption the delay times (only for pellets where elapsed time is larger then 8 ms) are plotted against the reciprocal of the pellet velocity and a linear

function is fitted on the data (Fig.2.a). The vertical lines over plotted represent the typical error of the individual delay times calculated from the estimated uncertainty of the reconstruction of the separatrix surface ( $\pm 1\text{cm}$ ), the spatial calibration of the images ( $\pm 0.5\text{cm}$ ), the calculation of the time when the pellet crossed the separatrix ( $\pm 20\mu\text{s}$  for  $V_P = 240\text{m/s}$ ,  $\pm 10\mu\text{s}$  for  $V_P > 240\text{m/s}$ ), and determination of the reference ELM onset time ( $\pm 10\mu\text{s}$ ). It is obvious that beside the time of flight part a clear  $50\mu\text{s}$  delay time is observed. From the slope of the linear function the position of the seed perturbation can be calculated. We got that it is in the middle of the pedestal region of the plasma. Knowing the intrinsic delay time, the position of the seed perturbation can be calculated for every individual pellet. This can be seen on Fig. 2.b. where the plasma pressure profile is plotted together with the histogram of the calculated position of the seed perturbation. It is again the case that the most probable position of the seed perturbation is in the middle of the pedestal and the full half width is about of one third of the whole pedestal.

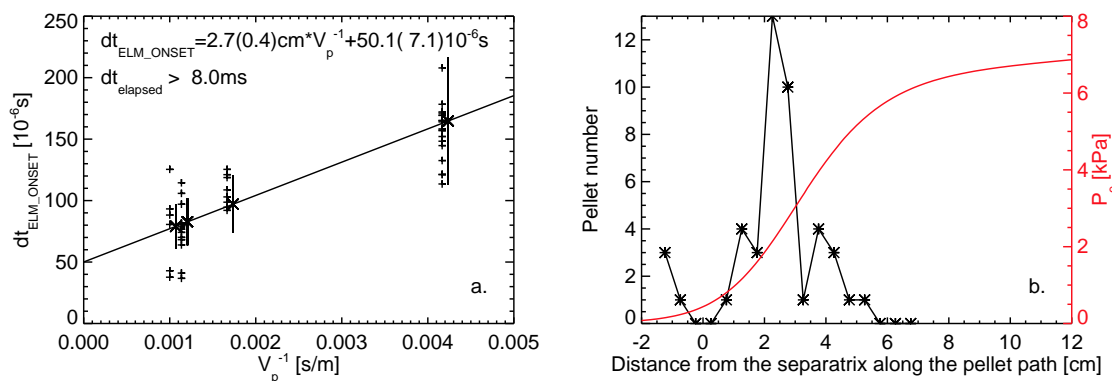


Fig.2. ELM onset delay time as a function of the inverse pellet velocity for elapsed time larger than 8ms (a) and the accordingly calculated histogram of the location of the seed perturbation (b). The typical plasma pressure profile is also plotted.

## References

- [1] A. Deggeling et al *Plasma Phys. Contr. Fusion* **45**, 1637 (2003)
- [2] P.T. Lang et al *Plasma Phys. Contr. Fusion* **47**, 1495 (2005)
- [3] P.T. Lang et al *Nucl. Fusion* **43**, 1110 (2003)
- [4] P.T. Lang et al *Rev. Sci. Instrum* **74**, 3974 (2003)
- [5] S. Kálvin et al *Europhysics Conference Abstracts*, Vol. 29C, P-2.078
- [6] P.J. Mc Carthy et al *IPP Report 5/85* Max-Planck-Institut fur Plasmaphysik, Garching, Germany (1999)
- [7] T. Bolzonella et al *Plasma Phys. Contr. Fusion* **46**, A143 (2004)
- [8] M. Schittenhelm et al *Nucl. Fusion* **37**, 1255 (1997)
- [9] N.E. Huang et al *Proc. R. Soc. Lond. A* **454**, 903 (1998)